

EXPERIMENTAL STUDY OF HEAT-AND-MASS TRANSFER IN CONTACT STEAM-AND-SMOKE MIXTURE GENERATOR

M. N. Nikitin

Samara State Technical University, Samara, Russia

1. Introduction

Multi-component heat carriers, in particular steam-and-smoke mixtures (SSM), currently promising low cost alternatives to water vapor with similar enthalpy and other crucial parameters. The temperature of steam-and-smoke mixtures can reach 800°C , with constant pressure approximately 0.1 MPa. Due to specifics of SSM generation, the mechanism is almost independent of generator capacity. [1]

SSM are used as heat carriers in many industries. A variety of its applications is determined by low cost and simplicity of generation. SSM generators are used for cleaning surfaces and tanks from thick liquids (oils and its residues). They are also used for lubeoil removal from equipment and defrosting of valves during winter season. Steam-and-smoke mixtures can also be used for timber and concrete curing.

Low requirements toward feed water quality and mobility of SSM generators made them a very popular substitute for traditional steam boilers in agriculture. Several farms use SSM for thermal sterilization of soil and disinfection of barns.

Steam-and-smoke mixtures are generated in the mixing heat generators by spraying pre-heated water into a stream of combustion products of gaseous fuel. Evaporation of sprayed droplets results in vapor phase, which mixes with the flue gases and forms a homogeneous multicomponent stream [2]. Flow rate of injecting water determines outlet temperature of SSM *ceteris paribus*. That basic correlation for temperature range $100\div 600^{\circ}\text{C}$ represented in Table 1.

Table 1

SSM characteristics for liquid gas (butane)

$T_{SSM}, ^{\circ}\text{C}$	$G_w, \text{kg}/\text{Nm}^3$	$G_{SSM}, \text{kg}/\text{Nm}^3$	$G_{SSM}, \text{m}^3/\text{Nm}^3$
100	45.42	103.79	122.67
200	42.19	100.56	149.66
300	39.40	97.77	173.88
400	36.94	95.31	197.87
500	34.64	93.01	160.29
600	32.58	90.95	237.24

Table 1 shows required specific flow rate of injecting water per normal cubic meter of butane. Mass and volume flow rates of steam-and-smoke mixture are also specified per normal cubic meter of butane. One can see that volume flow rate of SSM dramatically increases with its outlet temperature while mass flow rate slightly decreases. This effect caused by volume expansivity of gases and should be considered due to near atmospheric pressure of SSM [1].

A mathematical description of SSM generation is rather sophisticated: in addition to volume heat and mass transfer it's necessary to consider probability factors (for example, when calculating the spectrum geometry of droplets spray), while computational solution requires initial successive approximation [3]. Experimental study was conducted to investigate regime factors influence on the process of SSM generation and its parameters.

2. Experimental study

Experimental setup (Fig. 1) with heat capacity of 4 kW contains all crucial elements that are present in generators of this type [4]. Combustion chamber 3 made of two perpendicular cylinders and contractor. Heat liberation of combustion chamber shouldn't exceed recommended value, otherwise incomplete combustion could happen. Mixing chamber 5 formed as Venturi tube for optimal SSM generation process. Diffuser of mixing chamber preferably has divergence angle of $8\div 12^\circ$ to provide optimal dynamics of SSM pressure and velocity.

Injection device 1 made of coaxial cylinder and contractor with atomizer 6. Water injection occurs at Venturi neck, where flue gases have maximum velocity and minimal static pressure. Atomizer generates fine water spray (mist) with microscopic droplets. Small diameter of generated droplets means rapid evaporation without precipitate particles on walls of mixing chamber.

SSM generator equipped with adjustable liquid butane burner with capacity of 4 kW.

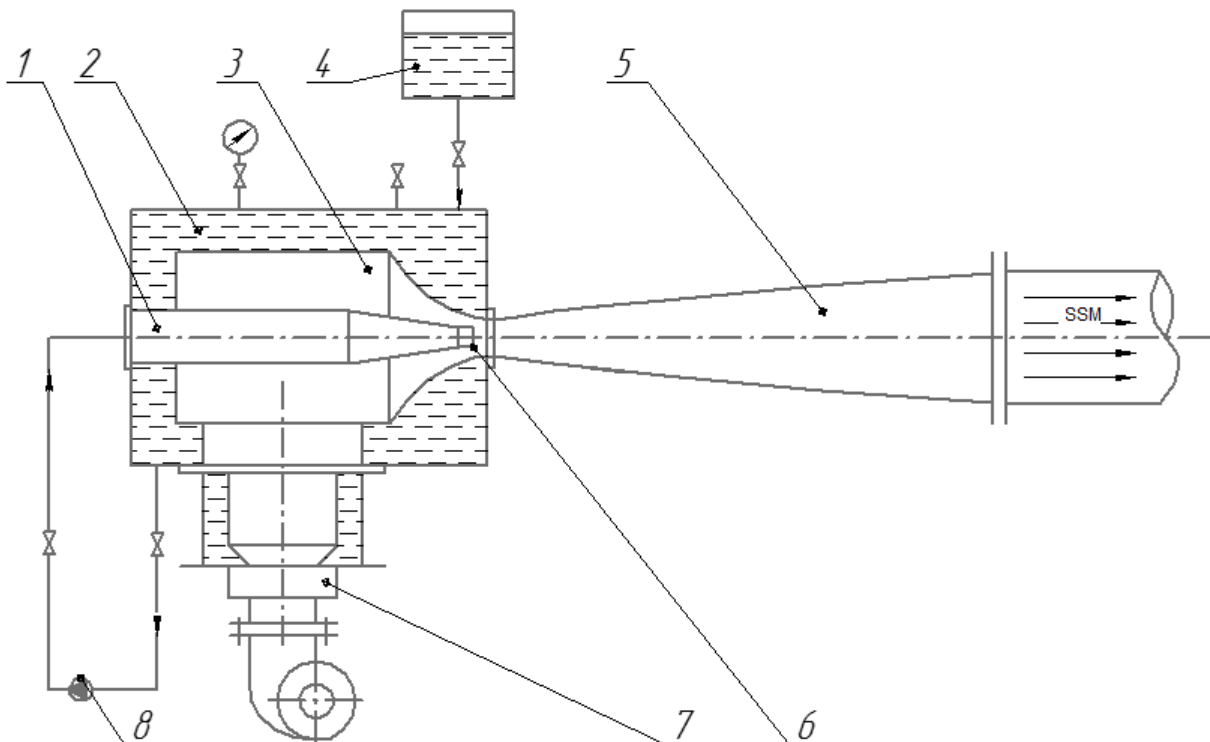
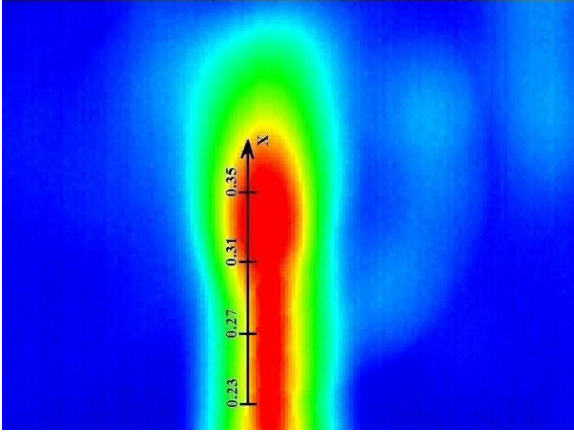
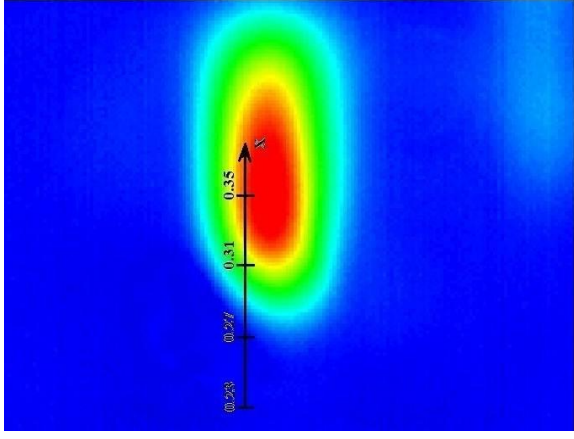


Fig. 1. SSM generator: 1 – injection device; 2 – cooling casing of combustion chamber; 3 – combustion chamber; 4 – storage container; 5 – mixing chamber; 6 – atomizer; 7 – burner; 8 – water pump

Four series of experiments corresponding to various operational conditions were conducted: (I) with variable temperature of injecting water ($T_w = 10\div 60^\circ\text{C}$); (II) with various flow rate of injecting water ($G_w = 2.4\div 42.5$ kg/h); (III) with various burner capacity ($N = 2\div 4$ kW); (IV) with various offset of the injection point ($\Delta x = -0.02\dots+0.02$ m). Each one consists of six runs, documented with infrared camera MobIR M4.

To obtain visibility of SSM flow on infrared images, net screen used. Square netted screen is made of stainless steel wire ($\varnothing 25$ mm) with 1 mm step. Screen diameter is 0.24 m (452 cm²). Calibration of infrared camera made by measurement of net screen temperature with digital thermometer Leybold Didactic GmbH equipped with NiCr-Ni thermocouple probes. Calibration test determined emissivity factor of net screen ($\varepsilon = 0.16$) which confirmed by recommended range for polished stainless steels ($\varepsilon = 0.12\div 0.2$).

Infrared images (Fig. 2 – Fig. 5) show temperature fields of SSM stream and diagrams of temperature maximums distribution.



3

Fig. 2. Infrared image from the 1st series of experiments ($T_w = 60^\circ\text{C}$)

Fig. 3. Infrared image from the 2nd series of experiments ($G_w = 42.5 \text{ kg/h}$)

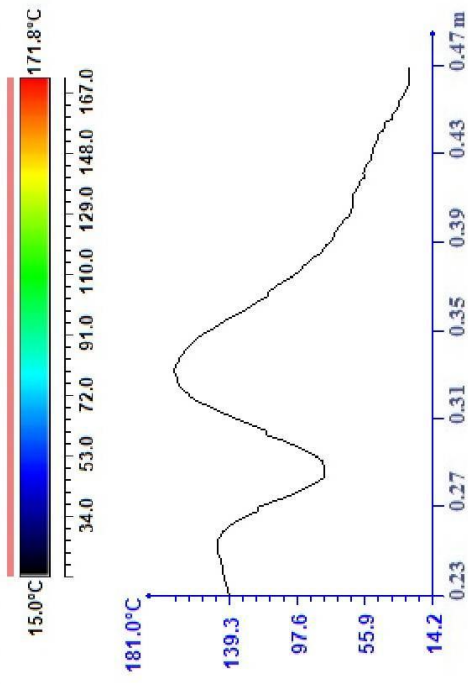
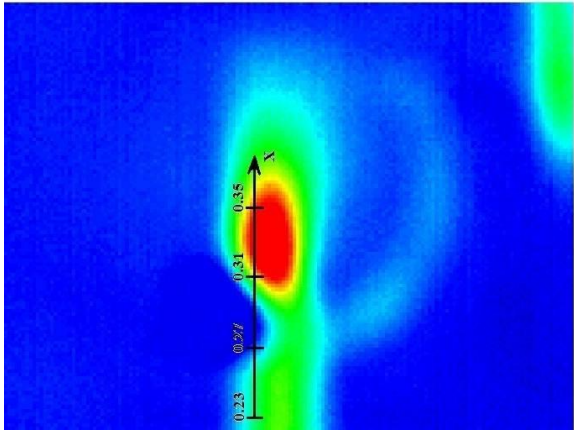
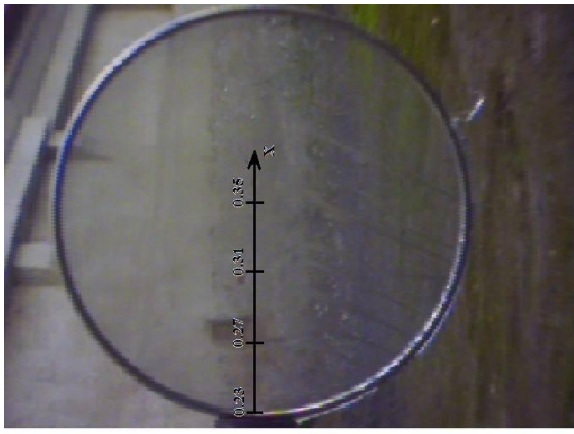


Fig. 5. Infrared image from the 4th series of experiments ($\Delta x = +0.02$ m)

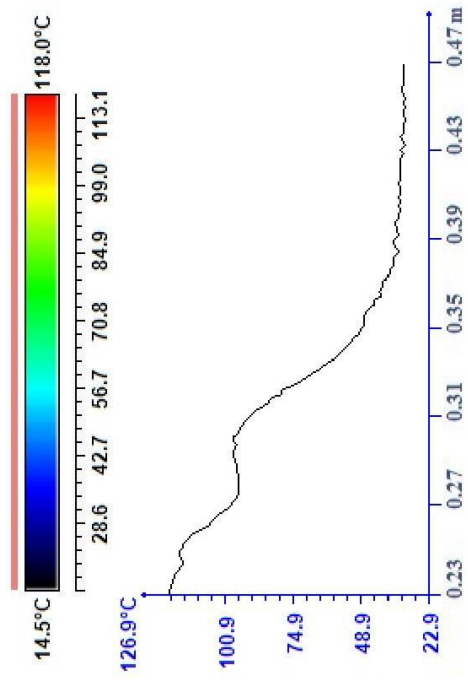
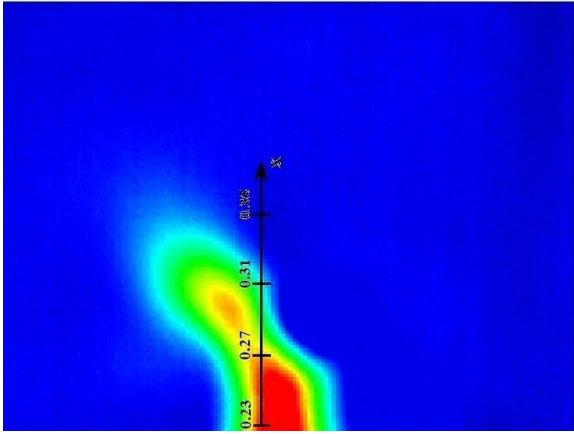


Fig. 4. Infrared image from the 3rd series of experiments ($N^{nom} = 2$ kW)

Experimental data for each series of experiments were processed with Student's distribution for the analysis of measurement accuracy (Table 2). The analysis conducted for experimental data for which Cochran criterion didn't exceed the critical value. This confirmed the independence of the temperature at each point of its absolute value [5].

Table 2

Processed experimental data of the 1st series of experiments ($T_w = \text{var}$)

$T_w, ^\circ\text{C}$	10	20	30	40	50	60
$T_{SSM(X=0.23)}, ^\circ\text{C}$	142.843 ± 0.86	159.400 ± 0.95	174.643 ± 1.10	189.329 ± 0.91	206.500 ± 0.94	221.486 ± 0.75
$T_{SSM(X=0.27)}, ^\circ\text{C}$	134.757 ± 0.82	149.514 ± 0.95	165.614 ± 0.93	179.686 ± 0.76	195.529 ± 0.97	210.771 ± 0.77
$T_{SSM(X=0.31)}, ^\circ\text{C}$	128.700 ± 0.83	143.471 ± 0.90	158.343 ± 0.87	173.600 ± 0.69	189.600 ± 0.99	205.543 ± 0.72
$T_{SSM(X=0.35)}, ^\circ\text{C}$	120.329 ± 0.94	135.571 ± 0.90	151.243 ± 0.97	166.443 ± 0.84	181.386 ± 0.97	196.829 ± 0.94

The 1st series of experiments (Table 2) conducted under the following conditions: burner capacity $N = 4$ kW; injected water flow rate $G_w = 4.6$ kg/h; pressure of injected water $P_w = 0.065$ MPa; offset of the injection point $\Delta x = 0$ m; ambient temperature $T_o = 28^\circ\text{C}$. The temperature of condensate for the 1st series of experiments didn't change significantly and was $92 \pm 4.4^\circ\text{C}$.

Experimental data of the 1st series of experiments appeared to be in sufficient convergence with the results of mathematical modeling. Modeling adequacy confirmed with the Fisher criterion, which is defined as the ratio of adequacy variance to error mean square. For the 1st series of experiments, $F = 0.75$ for the critical value $F_{cr} = 1$.

Table 3

Processed experimental data of the 2nd series of experiments ($P_w, G_w = \text{var}$)

P_w, MPa	0.05	0.1	0.15	0.2	0.25	0.3
$G_w, \text{kg/h}$	2.20	10.26	18.32	26.39	34.45	42.52
$T_{SSM(X=0.23)}, ^\circ\text{C}$	149.586 ± 0.78	127.543 ± 1.08	105.700 ± 0.96	83.743 ± 0.71	60.514 ± 1.05	37.786 ± 0.89
$T_{SSM(X=0.27)}, ^\circ\text{C}$	130.529 ± 0.92	112.543 ± 0.99	94.700 ± 0.86	76.743 ± 0.93	58.486 ± 0.96	40.057 ± 0.88
$T_{SSM(X=0.31)}, ^\circ\text{C}$	143.443 ± 0.94	133.286 ± 0.84	124.071 ± 0.54	115.786 ± 0.88	105.400 ± 0.83	97.743 ± 0.85
$T_{SSM(X=0.35)}, ^\circ\text{C}$	181.500 ± 0.64	174.400 ± 0.94	167.757 ± 0.95	159.657 ± 0.79	151.586 ± 1.10	145.686 ± 0.99
$G_{exc}, \text{kg/h}$	–	6.01	15.01	24.01	33.01	38.99
$T_{exc}, ^\circ\text{C}$	–	90	80	70	60	50

The 2nd series of experiments (Table 3) conducted under the following conditions: burner capacity $N = 4$ kW; injected water temperature $T_w = 10^\circ\text{C}$; offset of the injection point $\Delta x = 0$ m; ambient temperature $T_o = 28^\circ\text{C}$. Increasing of injected water flow rate over its critical value $G_w^{cr} = 4.6$ kg/h (for described conditions) results in occurring of excessive water in mixing chamber of generator. Further increasing of injecting water flow rate results in steady increasing of excessive water flow rate G_{exc} while decreasing its temperature T_{exc} .

Approximate flow rate of non-evaporated water can be estimated with the following expression:

$$G_{exc} = 1.116(G_w - G_w^{cr}).$$

Table 4

Processed experimental data of the 3rd series of experiments ($N^{nom} = \text{var}$)

N^{nom} , kW	2	2.5	3	3.5	4
$T_{SSM(X=0.23)}$, °C	117.686 ±0.82	123.857 ±0.82	128.614 ±0.94	133.743 ±1.01	138.529 ±0.98
$T_{SSM(X=0.27)}$, °C	197.514 ±0.78	176.671 ±1.04	154.514 ±0.92	135.271 ±0.92	113.586 ±1.05
$T_{SSM(X=0.31)}$, °C	90.429 ±0.75	101.643 ±0.70	112.657 ±1.01	121.743 ±0.98	129.571 ±0.84
$T_{SSM(X=0.35)}$, °C	49.543 ±0.87	79.643 ±0.98	110.414 ±0.96	139.857 ±0.98	170.614 ±0.83
G_{exc} , kg/h	2.40	1.50	0.60	–	–
T_{exc} , °C	70	80	90	–	–

The 3rd series of experiments (Table 4) conducted under the following conditions: injected water flow rate $G_w = 4.6$ kg/h; pressure of injected water $P_w = 0.065$ MPa; injected water temperature $T_w = 10^\circ\text{C}$; offset of the injection point $\Delta x = 0$ m; ambient temperature $T_o = 28^\circ\text{C}$. Decreasing of burner capacity below 3.2 kW results in occurring of excessive water in mixing chamber of generator. Further decreasing of burner capacity results in steady increasing of excessive water flow rate G_{exc} while decreasing its temperature T_{exc} .

Approximate flow rate of non-evaporated water can be estimated with the following expression:

$$G_{exc} = 0.0025(N^{nom} - N).$$

Table 5

Processed experimental data of the 4th series of experiments ($\Delta x = \text{var}$)

Δx , m	-0.02	-0.01	0.00	+0.01	+0.02
$T_{SSM(X=0.23)}$, °C	140.043 ±0.91	139.943 ±0.97	140.300 ±0.95	139.771 ±0.89	139.813 ±0.92
$T_{SSM(X=0.27)}$, °C	115.657 ±0.88	115.843 ±0.85	115.971 ±0.95	115.243 ±0.76	115.716 ±0.89
$T_{SSM(X=0.31)}$, °C	131.486 ±0.97	131.614 ±1.06	131.957 ±1.05	131.414 ±0.96	131.556 ±0.99
$T_{SSM(X=0.35)}$, °C	172.500 ±0.83	172.714 ±1.07	172.829 ±1.08	172.343 ±1.06	172.567 ±0.97

The 4th series of experiments (Table 5) conducted under the following conditions: burner capacity $N = 4$ kW; injected water flow rate $G_w = 4.6$ kg/h; pressure of injected water $P_w = 0.065$ MPa; injected water temperature $T_w = 10^\circ\text{C}$; ambient temperature $T_o = 28^\circ\text{C}$. Variation of injection point position Δx doesn't result in significant SSM parameters alteration. This result was expected due to principle of SSM generation which is quite different from jet devices that use injection impulse.

3. Numerical modeling validation

Numerical modeling of SSM generator reveals correlations which characterize the process of steam-and-smoke mixtures generation. Results of modeling are shown on diagrams (Fig. 6 and Fig. 7). Solid graphs represent results of numerical modeling, while marks represent aggregated experimental data.

To achieve certain unification of obtained correlations, specific dimensions are used. For example, specific length of mixing chamber of SSM generator x/d represented in relation to its diameter (Fig. 6).

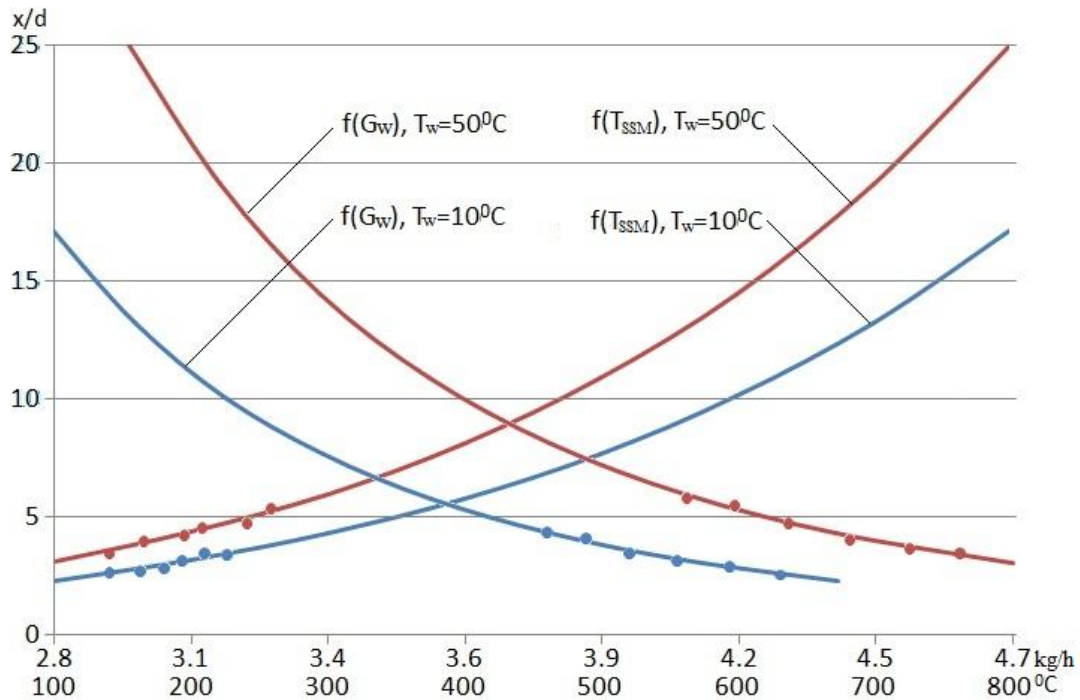


Fig. 6. Correlations between specific length of mixing chamber and SSM parameters

Correlations on Fig. 6 are calculated for 4 kW SSM generator. Axis of ordinates represents minimal specific length of mixing chamber of SSM generator x/d . Hence x/d represents the ending point of SSM generation process. Mixing chamber can be longer without any significant effect on SSM parameters, but this will result in bulky and heavy generator.

Solid graphs drawn from left to right (Fig. 6) represent correlations between specific length of mixing chamber and SSM temperature. Colored lines show correlation range for corresponding temperatures of injecting water ($T_w = 10\div 50^\circ\text{C}$). Expansivity of SSM in restricted volume of mixing chamber results in increasing of flow velocity. Hence the higher SSM output temperature requires longer mixing chamber.

Reversed solid graphs (Fig. 6) represent correlations between specific length of mixing chamber and flow rate of injecting water. Colored lines show correlation range for corresponding temperatures of injecting water ($T_w = 10\div 50^\circ\text{C}$). Increasing of flow rate of injecting water means lower SSM output temperature and its velocity. Hence the shorter mixing chamber required.

Fig. 7 shows correlation of injecting water flow rate and output SSM temperature. Colored lines show correlation range for corresponding temperatures of injecting water ($T_w = 10\div 50^\circ\text{C}$). Preheating of injecting water allow higher water flow rates while maintaining nominal temperature of output SSM.

Straight parallel lines (Fig. 7) show effect of preheating injecting water on SSM output temperature in range of water flow rates ($G_w = 24\div 36 \text{ kg/Nm}^3$). Specific flow rates calculated per normal cubic meter of natural gas.

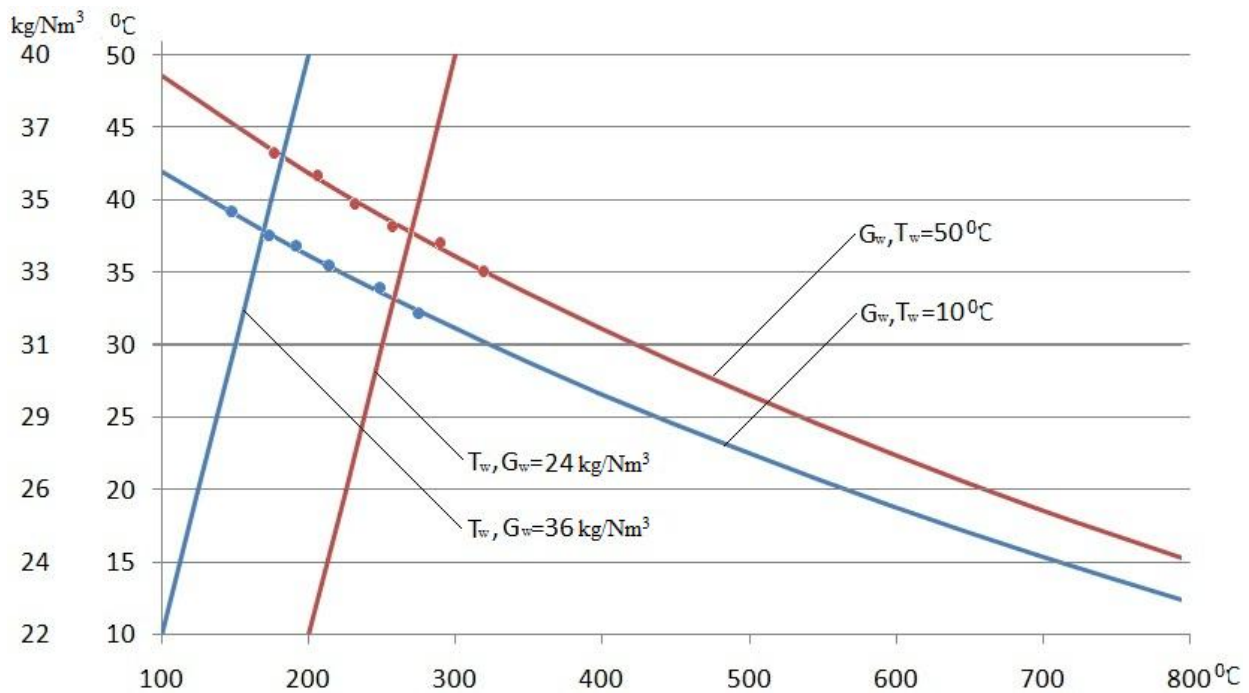


Fig. 7. Correlations between SSM temperature and regimes of its generation

4. Conclusions

Obtained empirical data and results of numerical modeling lead to the following conclusions:

1. Increasing of injecting water temperature and burner capacity results in higher output temperature of SSM, while excessive flow rate of injecting water results in SSM temperature drop and occurring of nonevaporable residue.
2. Increasing of SSM output temperature requires longer mixing chamber due to higher flow velocity.

Notation

T_w – temperature of injecting water, $^{\circ}\text{C}$; T_{SSM} – temperature of steam-and-smoke mixture, $^{\circ}\text{C}$; T_o – ambient temperature, $^{\circ}\text{C}$; G_w – mass flow rate of injecting water, kg/h; G_{SSM} – mass (volume) flow rate of SSM, kg/Nm³ (m³/Nm³); P_w – pressure of injecting water, MPa; N – burner capacity, kW; N^{nom} – nominal burner capacity, kW; x – distance from injection point towards the SSM flow, m; Δx – offset of the injection point, m; F_{cr} – critical value of Fisher criterion; G_{exc} – mass flow rate of excessive (nonevaporable) injecting water, kg/h; T_{exc} – mass temperature of excessive (nonevaporable) injecting water, $^{\circ}\text{C}$.

References

1. Nikitin M.N. The effect of directional water injection in the power generator on the pressure of obtained vapor-gas mixture, *Industrial Energy*, 2010, No 6, pp. 42–46.
2. Nikitin M.N., Shchelokov A. I., inventors. 2010 Aug. 10. Steam generator. Russian Federation patent RU 2,396,485.
3. Mostinsky I.L. et al. Cooling high-temperature gas in washer, *Industrial Heat Engineering*, 1980, No 3, pp. 96–103.
4. Amelin Engineering: Design and operation [cited 2012 Jan. 26]. URL: http://www.amelin.ca/eng/design_operations.htm.
5. Lemeshko B.Y. Statistical analysis of univariate observations of random variables. Novosibirsk: NSTU Press, 1995.